17
Higher Order Chromatin Organization and Dynamics

Hilmar Strickfaden, Thomas Cremer, and Karsten Rippe

17.1
Introduction

A century ago Theodor Boveri (1862–1915) proposed several bold hypotheses with regard to the organization and dynamics of chromosomes (for reviews, see [1–3]): (i) chromosomes maintain their individuality in cycling cells and are confined to distinct nuclear regions, called chromosome territories (CTs), (ii) arrangements of these CTs are stably maintained during interphase, (iii) chromosome proximity patterns change profoundly during prometaphase, (iv) similar CT arrangements in pairs of daughter nuclei reflect symmetrical chromosomal movements during anaphase and telophase, and (v) CT proximity patterns in daughter nuclei differ substantially from the mother cell nucleus, whereas radial chromatin arrangements are maintained. Boveri based these hypotheses on his studies of early cleavage stages of fertilized *Parascaris equorum* eggs (or *Ascaris megalocephala* as the horse roundworm was called in Boveri's days). Since individual chromosomes could not be visualized in interphase nuclei at Boveri's time, he took advantage of nuclear blebs (*Kernfortsätze*), which carry one or several chromosomal ends during the early blastomere stages of *P. equorum*. These blebs served as markers for the nuclear positions of Boveri's hypothetical CTs. During the 1970s and 1980s compelling evidence for CTs was obtained first by UV microirradiation experiments and then by chromosome painting (for a review, see [4]). Recently, live-cell imaging has provided strong evidence in favor of Boveri's further hypotheses [5].

Electron microscopic studies of the nucleus starting in the 1950s provided the first important insights into nuclear organization [6–15], yet failed to discover the territorial organization of chromosomes in the cell nucleus. The quite extensive early attempts to prove non-random arrangements of chromosomes in metaphase spreads are reviewed in Ref. [9]. Only recently, approaches for detailed studies of CT structure and arrangements in nuclei of fixed and living cells became available that combine molecular cytogenetics, molecular biology, and advanced light and electron microscopy. Furthermore, the *zeitgeist* was not favorable to encourage and fund such research extensively at a time when molecular biology alone seemed capable to unravel the mechanisms for nuclear functions, such as

Genome Organization And Function In The Cell Nucleus, First Edition. Edited by Karsten Rippe.

Published 2012 by WILEY-VCH Verlag GmbH & Co. KGaA

chromatin replication, gene expression, and DNA repair. This attitude has changed since it has become obvious that higher order chromatin organization matters for the regulation of nuclear functions. A wealth of information on functional chromatin organization in cell nuclei from various cell types and species has provided an increasingly detailed and quantitative insight into the dynamic organization of chromatin in the cell nucleus (for reviews, see [3, 6, 11–16]). This chapter reviews the current state of knowledge on higher order structure and the dynamic arrangement of chromatin in the viscous liquid of normal diploid cell nuclei during the interphase of the cell cycle. During mitosis chromosomes reorganize into highly compacted structures, as described in Chapter 18.

17.2 Higher Order Chromatin Organization: From 10-nm Thick Nucleosome Chains to Chromosome Territories

The diploid genome of a normal, somatic mammalian cell nucleus comprises about 6×10^9 basepairs (bp) in the G1 phase of the cell cycle. In a male human cell nucleus, for example, this genome is organized in 22 autosomes and the gonosomes X and Y. The DNA content of individual chromosomes ranges from 47 to 247 megabasepairs (Mb) in G1 and doubles during S-phase. Mammalian cell nuclei with typical diameters in the range of 10–20 μm contain about 2 m of DNA in G1 and 4 m in G2 wrapped around histone octamers. This nucleoprotein complex is called the nucleosome and represents the basic building block of chromatin. As described in Chapter 3 the nucleosome consists of 145–147 bp of DNA wrapped around a histone octamer protein core. It has a cylindrical shape of 11 nm diameter and 5.5 nm height. The nucleosome repeat length (NRL) varies between 165 and 220 bp of DNA depending on the species and also on the cell type within a given organism. It amounts to about 200 bp in mammals. Accordingly, about 6.4 Gb or 7 pg DNA in a mammalian cell nucleus are assembled into $\sim$30 million nucleosomes. Two extreme levels of chromatin organization have been verified in cell nuclei of most eukaryotic species: the 10-nm thick "beads on a string" of nucleosomes [17] and the chromosome territories [11]. Higher order chromatin organization in between these two extreme levels has remained a matter of conflicting opinions [18–20]. The folding of the chain of nucleosomes is discussed in detail in Chapter 6 and the most relevant structural motives are summarized in Table 17.1.

Since the nucleosome chain (or fibers formed from it) can be considered as a polymer if sufficiently long, numerous models have been proposed that attempt to rationalize genome organization from polymer properties (see also Chapters 9 and 20). These are compiled in Table 17.2. It is noted that all of them are able to rationalize certain experimental results. However, currently no "unified" consensus chromatin polymer model exists that is suited to explain all essential features of chromosome organization that have been derived experimentally. In order to classify the hierarchical organization of chromosomes during interphase as

Table 17.1 Structural motives of nucleosome chain folding.

Structure	Description	References
10-nm fiber	Extended and fully unfolded nucleosome chain that has been proposed to exist also as the dominating conformation during interphase	[17, 20, 21]
Nucleosome "superbeads"	Eight (chicken and rat liver) to 48 nucleosomes (sea urchin sperm) associate into a globular particle	[22]
30-nm fiber	Chain of nucleosomes can reversibly fold into a fiber with a diameter of approximately 30 nm	[17, 23–25]
100-nm fiber	Compaction of 10-nm/30-nm fibers into "chromonema" fibers of 100–130 nm in diameter	[26–28]

Table 17.2 Polymer models proposed for chromatin organization.

Polymer model	Description	References
Random coil	Nucleosome chain folding is that of a polymer confined by the available nuclear space	[29]
Polymer melt	Resolution of nucleosome chain folding into a more homogenous liquid phase-like aggregate of nucleosomes devoid of periodic structure	[20, 30, 31]
Reptated polymer	Polymer mobility is reduced by a crowded network-like environment so that translocations of a locus at the polymer are reduced or "reptated" as compared to a homogenous solvent	This chapter
Entangled polymer	Chromosome territories arise from entanglement of nucleosome chain	[32]
Kinked polymer	Chromatin fiber with about 10 kinks per 1 Mb	[33]
Looped polymer	Loops of regular size that are tethered to a backbone-like structure	[34–36]
Multi-loop subcompartment (MLS)	The 30-nm fiber forms loops of roughly 100 kb that are arranged into rosettes	[37–40]
Random loop (RL)	Self-avoiding random walk folding of the chain with loops of a broad size range	[41, 42], Chapter 20
Fractal globule	Knot-free polymer conformation that enables maximally dense packing	[43, 44]

Table 17.3 Genome compartments.

Structure	Description	References
1 Mb chromatin domain (CD)	Higher order chromatin structure with a DNA content in the order of 1 Mb. Presumably built up from ~100-kb looped subdomains	[13, 45, 46] [47–50]
Perichromatin region (PR)	100–200 nm zone at the periphery of ~1-Mb CDs. Nuclear compartment most active for transcription, splicing, DNA replication, and repair	[12, 51, 52]
Chromosome territories (CT)	Chromosomes occupy distinct territories in nuclei of both interphase and postmitotic cells	[6, 11–13, 53–56]
Interchromatin compartment (IC)	A 3-D system of channels and lacunas expanding between CDs. It connects to nuclear pores and contains splicing speckles and nuclear bodies. While soluble nuclear proteins can freely exchange between the IC, the PR, and the interior of CDs, diffusion of large complexes appears constrained depending on size and electric charge. A potential role of the IC and/or PR as routes for mRNA needs to be further substantiated	[11–13, 57, 58]
Interchromosome domain (ICD)	Space preferentially expanding between CTs that is more easily accessible to large nuclear complexes than regions within the CTs. When the ICD model was first proposed, the sponge-like structure of CT with highly complex CT surfaces was not established. Instead, threshold boundaries of painted CTs were considered as delineating CT surfaces. Accordingly, it was wrongly assumed that RNA transcripts and splicing components were generally excluded from the CT interior.	[55, 59–64]
Interchromatin network (ICN)	Chromatin as a fiber network that is stabilized by intrachromosomal linkages	[56, 65]

observed in fluorescence and microscopy, different compartments and organizational principles have been proposed that are summarized in Table 17.3.

According to the chromosome territory–interchromatin compartment (CT-IC) model CTs are built up from higher order chromatin domains (CDs) with an average DNA content in the order 1 Mb DNA [13] (Figure 17.1). These ~1-Mb CDs represent basic structural units of CTs and can be visualized during S-phase as replication foci in living cells after the incorporation of thymidine analogs directly conjugated to certain fluorophores [45]. While their mean diameter was first estimated to be in the order of 500 nm, recent measurements yielded much smaller values between 40 and 210 nm [46]. The ~1-Mb CDs are interconnected by chromatin fibers and may be built up from smaller chromatin loop domains with ~100 kb DNA content (~100 kb CDs). The scheme in Figure 17.1b exemplifies small chromatin loops representing the decondensed chromatin of transcribed genes (indicated by dashed black circles). Narrow IC channels may be filled

by small-sized chromatin fibers/loops ($\leq$200 nm), allowing direct contacts in *cis* and *trans*, that is, between CDs belonging to the same CT and to neighboring CTs, respectively (Figure 17.1b, dashed blue circle). The contacts are promoted by the transient translocation of CDs due to constrained Brownian motions. Non-random connections between chromatin occur both in *cis* within a given CT, and in *trans* between different CTs yielding a 3-D higher order chromatin network expanding throughout the nuclear space [46]. This network is involved in establishing and maintaining a stable 3-D but at special occasions also dynamic 4-D (space and time) organization of nuclear chromatin [5, 57] (see Sections 17.6 and 17.7). The CT-IC model argues for an interchromatin compartment (IC) with channels and lacunas extending not only between CTs but also extensively permeating into their interior [11, 13]. The IC is rich in ribonucleoproteins and harbors splicing speckles, as well as nuclear bodies [57]. Electron microscopic studies performed by Stan Fakan and co-workers have provided strong evidence for both the IC and a zone of decondensed chromatin, called the perichromatin region (PR), which exists at the periphery of $\sim$1-Mb CDs and is now considered as an essential subcompartment for transcription, co-transcriptional splicing, DNA replication and possibly also DNA repair [12, 51, 52]. In a recent study, 3-D structured illumination microscopy (3D-SIM) and spectral precision distance microscopy (SPDM) were combined to examine the nuclear topography of DNA, nascent RNA, and nascent DNA, as well as RNA polymerase II (RNA Pol II) and histone modifications typical for transcriptionally competent/active chromatin, such as H3K4me3 and H4K8ac [71]. The 3D-SIM observations demonstrate a strong enrichment of these components in the PR and a lack both in IC lacunas and the interior of CDs.

Evidence obtained with SPDM confirmed the presence of RNA Pol II clusters indicative of transcription factories. In contrast, the interior of CDs lacks such markers as well as nascent RNA and DNA. Interestingly, an electron microscopic study revealed that silencing proteins coded by polycomb group genes are also concentrated in the PR of the mammalian nucleus [68]. However, the results of Ref. [72] also suggest that a substantial part of transcription takes place in RNA Pol II outside such factories. We hypothesize that the functional nuclear organization of transcription and DNA replication depends on dynamic interactions between the transcriptionally engaged chromatin located in the PR, the transcriptionally silent chromatin located in the interior of CDs and the IC, as a storage site for the supply of essential proteins, as well as RNA export. In summary, CTs may be compared with sponges consisting of a network of $\sim$1-Mb CDs and bigger domain clusters permeated by IC channels [57, 58]. An earlier model of nuclear architecture, called the ICD model, argued that transcription should occur mostly in an interchromatin domain (ICD), which mainly expands between neighboring CTs [55, 59]. Accordingly, this model predicted that transcription occurs mostly at the periphery of CTs, whereas the CT-IC model takes into account that transcription can take in the PR both inside and in the periphery of a given CT.

Direct contacts in *cis* and *trans* are emphasized by the interchromatin network (ICN) model [72]. This model suggests much larger intermingling chromatin

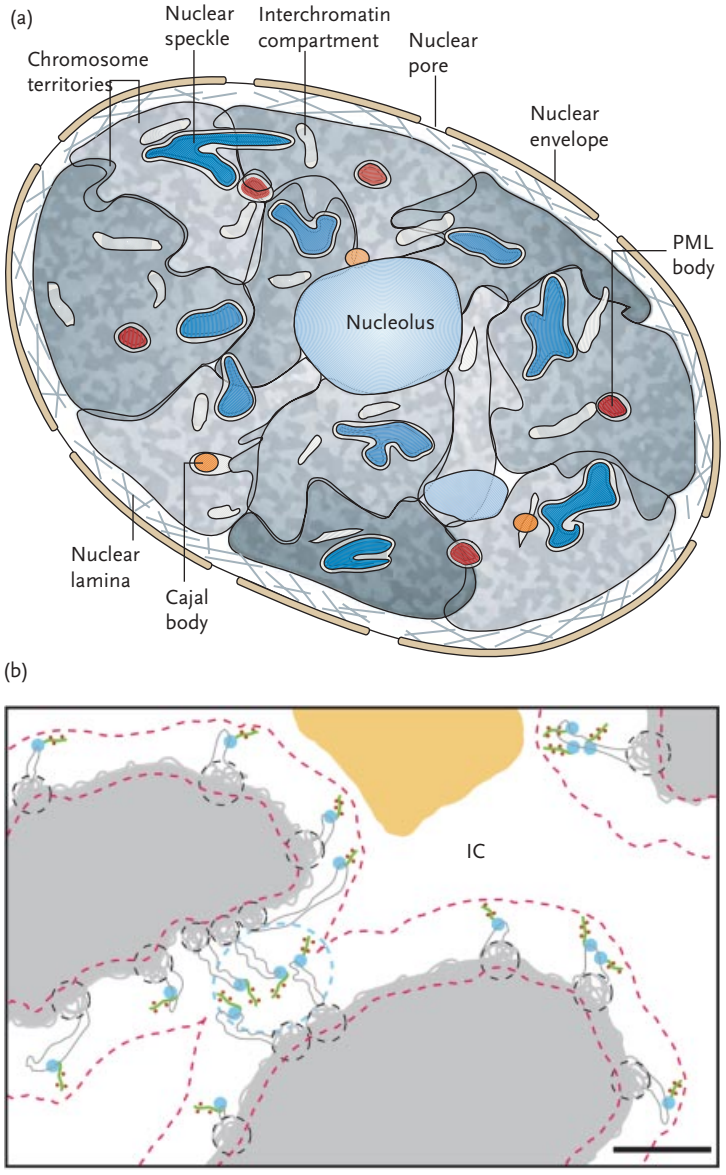

fibers than the CT-IC model to explain the relatively large regions of chromatin overlap observed between neighboring CTs. It dismisses the IC and PR as structurally and functionally distinct nuclear compartments [72]. Instead, it argues that machineries for major nuclear functions can be formed within the interchromatin space present between extensive intermingling of chromatin fibers and large loops in the interior of CTs and in border zones of neighboring CTs driven by Brownian

Figure 17.1 Structural and functional nuclear organization according to the chromosome territory-interchromatin compartment (CT-IC) model. (a) Schematic section through a mammalian cell nucleus (scheme modified from ref. [16]). Various nuclear compartments are depicted that include nucleoli, chromosome territories and the interchromatin compartment (IC). The IC starts/ends at nuclear pores and pervades the nuclear space as a system of channels and lacunas expanding both at the periphery of CTs and throughout their interior. The scheme shows the entire IC network as low density chromatin regions in light gray and emphasizes cross sections through larger chromatin free lacunas. These harbor nuclear bodies, such as PML bodies and Cajal bodies, as well as splicing speckles [66, 67]. It is important to note that neighboring CTs are not fully separated from each other by an interchromosomal domain (ICD) as previously suggested [55, 59], but reveal many sites of mutual, direct chromatin contacts. (b) Hypothetical view of the functional nuclear architecture at larger magnification (scale bar: 200 nm). CTs are built up like a sponge from chromatin domains (CDs) and the pervading IC. Its local width varies from smallest channels ($\leq$100 nm) to lacunas ($>$400 nm). Electron microscopic studies [68–70], supplemented by super-resolution fluorescence microscopy [71], indicate that fundamental nuclear functions such as transcription, co-transcriptional splicing, DNA replication and repair occur in the perichromatin region (PR) located at the periphery of CDs. It comprises a 100–200 nm thick zone of transcriptionally competent chromatin (marked by dashed red lines). In contrast, the core of CDs arguably carries silent chromatin. The CT-IC model predicts a major functional role of small-scale chromatin movements taking place between the PR and the core of CDs. Constrained Brownian movements of chromatin domains allow transient contacts between chromatin loops present in the PR.

motions. These would provide opportunities for intra- and interchromosomal rearrangements predicted to play a major role for the spatial congression of genes in *trans*. In contrast, the CT-IC model argues that giant loops crossing major parts of the nucleus are infrequent or may not exist at all (compare Figures 1.2 and 1.8 in [11] and Sections 17.6 and 17.7 below). Both the ICN model and the CT-IC model allow for the existence of a large non-chromatin space. However, the space between intermingling chromatin fibers/loops predicted by the ICN model should not be confused with the much more elaborated, structural, and functional organization of the IC and PR predicted by the CT-IC model.

Branco and Pombo reported that intermingling volumes between specific CTs correlate with the frequency of chromosome translocations after exposure to ionizing radiation [72]. Experimentally observed frequencies of chromosome translocations, however, are also in line with the CT-IC model [73, 74]. As a result of constrained Brownian movements of CDs, the width of IC channels between them is highly variable (see Section 17.4). Accordingly, two CDs, each carrying a single double strand DNA break (DSB), may approach each other close enough to enable aberrant ligations between broken DNA ends within the same repair machinery. The range of nuclear phenotypes reflecting the large variety of functional states is currently not well established. Possibly, the CT-IC model and the ICN model represent extreme examples of nuclear phenotypes. To address this issue, studies of cell nuclei with different gene expression patterns are necessary, ranging from nuclei which are transcriptionally inactive to nuclei with a high global transcriptional activity. Furthermore, nuclear architecture needs to be

evaluated in the context of the evolutionary development from unicellular eukaryotes to multicellular animal and plant species to distinguish features possibly conserved in all eukaryotes from species and cell type-specific peculiarities [14]. We expect that quite a number of unexpected and intriguing discoveries are waiting along this line of research. At present it is not clear at all whether a single model will finally suffice or whether such studies will support several models, reflecting profoundly different pathways of nuclear evolution.

17.3
Genome Accessibility

17.3.1
Chromatin Density Distributions and Accessibility of Nuclear Space

Chromatin contains histone proteins and DNA is present at a concentration of 7 mg ml^{-1} and 19 mg ml^{-1}. It would occupy $\sim$10% of the total nuclear volume when assuming its compaction into a 30-nm chromatin fiber with a mass density of 6–7 nucleosomes per 11 nm fiber contour length [75, 76] and somewhat less in an extended beads on a string structure, in which 0.5 nucleosomes are present per 11 nm of the chain. Some estimates on the accessibility of this fiber network can be made on the basis of nucleosome and/or DNA concentration measurements and experimental studies on the distribution of particles with different sizes in the nucleus. An average nucleosome concentration of 0.14 mM [77] or the equivalent of 18–19 mg ml^{-1} DNA ([78] and references therein) in a nuclear volume of 0.4 pl has been reported for mammalian cell lines. A bulk of the more densely packed heterochromatin has nucleosome concentrations of 0.2–0.3 mM with a small heterochromatin fraction ($\sim$10%) reaching a nucleosome density of 0.4–0.5 mM as inferred from fluorescence microscopy-based measurements [77, 79, 80]. It is noted that an only moderate twofold difference in terms of the density observed for euchromatin and bulk heterochromatin does not exclude higher compaction differences on a smaller length scale that are not resolved by optical methods. Consistent with this view, a tightly packed chromatin ultrastructure was revealed for the inactive X chromosome that was not apparent from a light microscopic comparison of the volume occupied by the inactive and active X chromosome [81]. Other heterochromatin domains visible on fluorescence microscopy images have dimensions in the micrometer scale and are mostly found at the nuclear periphery, around the nucleolus and at the centromeres. Reversible changes of the chromatin compaction state can be induced via factors like histone acetylation [79, 82], the induction of transcription [83], ATP depletion [57, 67], or by osmolarity variations of the medium [57],as discussed previously [57, 84].

During interphase, particles up to $\sim$20 nm in size experience no restrictions with respect to their nuclear distribution within the 200–300 nm lateral and about

800 nm axial resolution limit of light microscopy [79, 85, 86]. Particles with a size of ≥ 30 nm like 150 kDa and larger FITC-labeled dextrans are progressively excluded from dense chromatin regions. Particles with sizes around 100 nm (100 nm diameter nanospheres, 2.5 MDa dextrans) are completely excluded from the chromatin mesh [87, 88]. This is also relevant for CBs and PML-NBs with sizes of 0.1–1.0 μm, which therefore have access to a subspace of the nucleus only as discussed below.

17.3.2 Mobility of Inert Molecules and Complexes on Different Scales

From the considerations above it is apparent that mobility and accessibility of nuclear space are highly dependent on the size of a given particle. As a reference particle the 27-kDa green fluorescent protein (GFP) is frequently used. GFP has a barrel-like structure with a diameter of ~ 3 nm and a height of ~ 4 nm. It is uniformly distributed throughout the nucleus in fluorescence microscopy images without any apparent interactions with nuclear structures. The mobility of GFP has been well characterized in a number of studies by means of FCS and FRAP [86, 89, 90]. Its diffusion coefficient is 81 $\mu m^2\ s^{-1}$ in water at 25 °C with a viscosity of 0.89 mPa s. Average values of $D = 23\ \mu m^2\ s^{-1}$ were measured in the cell in the cytoplasm or nucleus. The difference to water can be assigned to an apparent 3.5-fold higher viscosity of the cellular environment. The cellular D value of GFP corresponds to an effective displacement of 12 μm after 1 s, which is similar to the dimensions of the cell nucleus. Thus, the time required for an isolated non-interacting protein molecule to "roam" the whole nucleus is in the range of a few seconds. GFP and dextrans of similar size have virtually unrestricted access to the whole nucleus at standard fluorescence microscopy resolution. Interestingly, also for larger particles like GFP pentamers with D as small as $8 \pm 1\ \mu m^2\ s^{-1}$ no differences in the diffusion coefficients were detected between the cytoplasm and the nucleoplasm [86]. As discussed in Chapter 7, the nucleoplasm represents an environment, in which macromolecules are highly concentrated. This effects both their interactions and their size-dependent mobility. Thus, inert particles up to a size of about ~ 20 nm experience no restriction with respect to their accessible space in the nucleus during interphase within the diffraction-limited resolution of the fluorescence microscope. In terms of protein mass, these dimensions would correspond to a molecular weight of 2–3 MDa. Accordingly, it is expected that in the absence of interactions with chromatin or other nuclear subcompartments, most nuclear factors are highly mobile. A compilation of experimental data that describe their mobility resulting from both diffusion and interactions can be found in Ref. [80]. With increasing size, macromolecules and complexes become increasingly excluded from nuclear areas of higher density [79] while they are still mobile. In contrast, dextrans, nanospheres, and inert NB-like complexes larger than 100 nm are trapped locally. However, they show some chromatin-embedded mobility (see below).

17.4
Mobility of Chromosomal Loci and Nuclear Bodies

17.4.1
Typical Mobilities of Genomic Loci

Compelling insights into the mobility of selected chromatin regions were obtained by tracking of labeled chromatin in living cells. Various methods were developed for this purpose. In an early study chromatin was fluorescently tagged using dihydroethidium, a membrane-permeant derivative of ethidium bromide [91]. After labeling, the authors used a laser microbeam to bleach small ($\sim$0.4 μm radius) spots in the heterochromatin and euchromatin of living Swiss 3T3 and HeLa cells. Observations of these spots indicated their persistence for >1 h suggesting that the bleached interphase euchromatin and heterochromatin was substantially immobile during the observation period. Other groups marked individual chromosomal loci in living eukaryotic cells, genomic sites by the integration of repetitive *lac* operator arrays, which were visualized with the help of LacI-GFP [92]. This approach was widely used to follow movements and conformational changes of chromatin (for a review, see [93]). By tracking tagged chromatin loci, average apparent diffusion coefficients of 1–2 10^{-4} μm^2 s^{-1} have been reported for chromatin loci and for large nuclear particle movements within a corral of 200–300 nm radius that can translocate in the nucleus as part of larger CDs [66] (Table 17.4). These relatively slow and confined movements are in agreement with a territorial organization of chromosomes and consistent with the slow mobility of broken chromatin ends formed after introducing a DNA cut [96]. Notably, the time regime chosen for the experiments directly affects the resulting apparent diffusion coefficients, if for example only the initial linear slope of the MSD versus time plot is evaluated [80].

Table 17.4 Mobility of chromatin loci in mammalian cells.

	Chromatin locus	Telomere/end[a]	Chromatin domain
D_{fast} (μm^2 s^{-1})	3 10^{-3}	1 10^{-3}	n. d.
$r_{c,fast}$ (nm)	70	80	n. d.
D_{slow} (μm^2 s^{-1})	2 10^{-4}	2 10^{-4}	n. d.
$r_{c,slow}$ (nm)	240	150	n. d.
D_{hour} (μm^2 s^{-1})	n. d.	1 10^{-5}	0.5–5 10^{-5}
References	[94, 95]	[96, 97–102]	[67, 98, 103]

D is the diffusion coefficient and r_c is the radius of confinement, that is, the effective radius of the region, within which a given particle or chromatin locus can translocate its center of mass during the observation time. Data acquired on different time scales suggest the existence of three regimes. At $t \leq 2$ s (D_{fast}), $t = 2$–10 s (D_{slow}) and $t \geq 1$ min (D_{hour}). The entry n. d. stands for "not determined".

[a]Average values observed for the majority of telomeres. A $\sim$10% fraction of telomeres showed a higher mobility, as discussed in the indicated references.

In a high resolution analysis the mobility of *lac*O arrays in CHO hamster cells and telomeres in the human U2OS cell line was measured on the second time scale [95, 98]. Multiple mobility layers were detected and the data could be fitted to a confined diffusion or "moving corral" model [80]. This analysis yielded $D_{\text{fast}} = 3.1\ 10^{-3}\ \mu m^2\ s^{-1}$ and $D_{\text{slow}} = 2.4\ 10^{-4}\ \mu m^2\ s^{-1}$ [95] and $D_{\text{sec}} = 2\ 10^{-3}\ \mu m^2\ s^{-1}$ and $D_{\text{min}} = 4\ 10^{-4}\ \mu m^2\ s^{-1}$ [98]. Interestingly, at the hour time scale, the diffusion coefficient $D_{\text{hour}} = 1\ 10^{-5}\ \mu m^2\ s^{-1}$ for telomeres or 1 Mb chromatin domains labeled with Cy3-UTP is much lower [98, 103]. This is in support of the view that this value represents the dynamics of large chromatin domains in the nucleus. The relatively low mobility measured for the majority of telomeres is also in agreement with a recent study where the mobility of DNA ends created from a double-strand break between a *lac*O/LacI-CFP and a *tet*O-TetR-YFP label was evaluated [96]. The results indicate that DNA ends per se do not display a higher mobility than other chromatin loci. This supports the model of a linked chromatin fiber network, in which the local chromatin mobility is confined to a radius of 150–250 nm [80]. In another study the telomere mobility in U2OS cells was analyzed over a time period of 30–60 min with 1 min time resolution after labeling the telomere repeats by hybridization with a PNA probe [102]. The majority of telomeres moved in a confined region with an apparent radius of ~ 0.5 μm and a short range diffusion coefficient of $1.8\ 10^{-4}\ \mu m^2\ s^{-1}$ as inferred from the plateau and initial slope of the MSD versus time plot. A $\sim 10\%$ fraction of telomeres displayed a higher mobility for which translocations up to 1.2 μm and an apparent diffusion coefficient of $5.8\ 10^{-4}\ \mu m^2\ s^{-1}$ were reported. In summary, the default mobility of a given genomic locus is rather low. While a radius of 100–200 nm is explored within seconds any translocation on the micrometer scale would typically require tens of minutes to hours. However, several instances of much faster long-range movements have been reported [104]. Their origin is of special interest since these could be important in the context of transcription-related chromatin reorganization [16, 105, 106]. This issue is reviewed in further detail below.

As a quantitative description for the average mobility of a genomic locus during interphase is depicted in Figure 17.2 using the data set from Ref. [98]. It shows the observed mobility of telomeres expressed as the mean squared displacement versus time over five orders of magnitude, that is, from milliseconds to hours. This relation can be evaluated according to a generalized diffusion model:

$$\text{MSD} = \langle d^2(\Delta t) \rangle = 2n\Gamma\Delta t^{\alpha}$$

in which n is the dimensionality and Γ is the transport coefficient. For $\alpha = 1$ it is equal the diffusion coefficient D and represents the case of simple diffusion. A fit of the telomere data set yields a value of $\alpha = 0.36$ when averaging over all data with $\alpha = 0.22$ for the fast times (t; up to 0.01 min) and $\alpha = 0.48$ for $t > 10$ min. This bears some striking similarity to the behavior of a polymer in a crowded environment or network according to the reptation model [107]. In this situation the polymer dynamics are characterized by a transition from the MSD being proportional to $t^{0.25}$ at short times and to $\propto t^{0.5}$ at longer times. Thus, on an averaged and global scale the dynamics of a chromatin locus can be described by

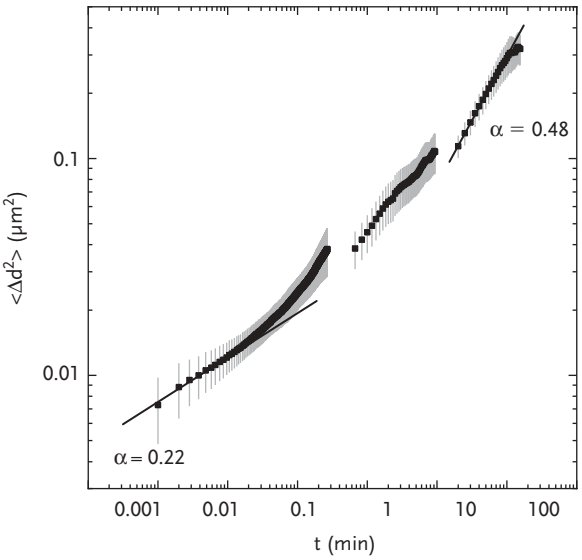

Figure 17.2 Dynamics of a chromosomal locus on a time scale from milliseconds to hours. The mean squared displacement versus time is plotted.

that of a polymer in a network that reduces its mobility. For a free polymer $\alpha = 0.5$ would be obtained [107]. Some features of this type of behavior were also reported in another study of telomere mobility over multiple time scales [99].

17.4.2 Mobility of Nuclear Bodies and Exchange of Protein Components with the Nucleoplasm

Both the structure and dynamics of CTs affect the location and mobility of nuclear bodies (NBs). These are mobile subcompartments in the nucleus and represent sites, in which specific genome-related activities are concentrated. It is an open question how these are targeted to a specific region of the nucleus [67, 108, 109]. NBs are dynamic structures that exchange their constituting components with the nucleoplasm on the scale of seconds to minutes as shown for Cajal bodies (CBs) [110], PML nuclear bodies (PML-NBs) [111], and speckles/SC35 domains involved in RNA processing [112, 113]. Thus, a mechanism for their translocation could be a highly dynamic fluid-like conformation that allows a transient disruption of its structure during passage through chromatin. At least in part this appears to apply for the very dynamic nuclear speckles/SC35 domains [113]. However, CBs and PML-NBs have a more stable structure that is mostly preserved during their translocations. This is apparent from the relatively high residence time of 48 min reported for the exchange of the PML V splicing variant between the freely mobile state in the nucleoplasm and a PML-NB complex [111]. This suggests that the structural scaffold of PML-NBs is relatively stable on this time scale.

Since CBs and PML-NBs have typical sizes of 0.1–1.0 μM diameter they are too large for an unrestricted movement. Accordingly, it was proposed that the dynamic chromatin organization of the interphase nucleus determines the confined translocation of mobile nuclear subcompartments like PML and Cajal nuclear bodies, and their targeting to certain regions of the nucleus [66, 67]. Consistent with this view nuclear bodies are highly enriched in the interchromatin compartment at the interface between chromosome territories [57]. The latter can be visualized via the polymerization of nuclear localization signal (NLS)-containing vimentin filaments [64, 66]. On the time scale of seconds to minutes or less, the movements of NBs can be described by a diffusion-like motion of the particles' center of mass in a corral with a radius of 200–300 nm that is at least transiently devoid of chromatin. This value is strikingly similar to what is observed for chromatin itself. Above this length scale a chromatin reorganization is required that allows the separation of chromatin subdomains in order to create accessible regions within and through the chromatin network. The associated chromatin locus translocations occur with an apparent diffusion coefficient of up to $\sim 10^{-4}$ μm^2 s^{-1} (Table 17.4). This is again similar to the value measured for nuclear bodies at the same time and length scales. The above view of the location and mobility of PML-NBs and CBs being determinants of the higher order chromosome structure and its dynamics does not account for the chromatin-bound states that these subcompartments can adopt. It has been shown that Cajal bodies are associated to several different snRNA and snoRNA (small nuclear/nucleolar RNA) gene loci as well as histone gene loci [114–118]. For PML-NBs an occasional association to certain gene regions [119, 120] as well as the formation of specific complexes with telomeres [121] has been reported.

17.5 Mitosis Causes Drastic Changes of Chromosome Territory Proximity Patterns in Cycling Cells

For many decades cell biologists lacked proper methods necessary to either confirm or falsify Boveri's hypothesis that CT arrangements established at the beginning of interphase are stably maintained throughout this interphase, whereas profound changes of such arrangements take place as a result of mitosis. In case of cycling cells, the question arises whether a given CT interphase arrangement can be propagated through the cell cycle. Several groups have studied this problem in living cells taking advantage of cell lines, which express core histones tagged with fluorescent GFP or RFP [122, 123], photoconvertible Dendra2 [124] or photoactivatable paGFP protein [5, 125]. By photobleaching, photoconversion or photoactivation via laser microirradiation distinct fluorescent chromatin patterns were established in interphase nuclei or on mitotic chromosomes. These patterns were then tracked through interphase and mitosis. Ellenberg and coworkers reported that global chromosome positions are maintained in cycling

mammalian cells despite major changes of prometaphase chromosome neighborhood arrangements [122]. A mechanism acting at anaphase was proposed to restore changes of chromosomal neighborhoods during prometaphase, but this report could not be confirmed in other studies. Walter *et al.* observed frequent examples, where chromatin arrangements in a mother nucleus differed drastically from the arrangements observed in daughter nuclei [123]. These authors also detected an increased chromatin mobility during the first 2 h of G1, which arguably provides a time window for the restoration of positional order. Thomson *et al.* used cell lines, in which stable integration of *lac*O arrays in different chromosomes were tracked via a bound GFP–LacI–NLS fusion protein [126]. These loci were followed from mitosis into daughter cell nuclei. The authors concluded that the organization of chromatin in the nucleus is not transmitted accurately from one cell to its descendants but is more plastic and becomes refined during early G1. In another study it was noted that the CT order present in daughter nuclei was strikingly different from the mother nucleus, although it was not entirely randomized [124]. Finally, Strickfaden *et al.* investigated these issues by transfecting the human cell-line RPE-1 simultaneously with a construct for H4 tagged with a photoactivatable GFP (paGFP) and another construct for H2B tagged with mRFP [5]. Various patterns of paGFP fluorescence were introduced and followed by live cell imaging through interphase and mitosis. Patterns produced in interphase nuclei typically persisted to the next prophase (see below for important exceptions from this rule). In contrast, the movements of prometaphase chromosomes involved in the formation of the metaphase plate resulted in new chromosomal neighborhoods, which were transmitted to the daughter nuclei. In conclusion, the weight of evidence supports Theodor Boveri's early hypotheses that CT neighborhood patterns are stably maintained during interphase, whereas mitosis leads to major changes of the pattern in cycling cells. These changes occur during prometaphase and are not restored during anaphase, in contrast to conclusions reported previously [122]. A single mitotic event might not be sufficient to yield a complete randomization of CT neighborhood arrangements in the two daughter nuclei: First, non-random radial arrangements of gene dense and gene poor CTs as well as some ordering of chromosomal subregions according to their gene density within a CT are maintained in cycling cells (Figure 17.3A). This constraints the possible range of changes with respect to CT neighborhood arrangements. Second, changes in neighborhood arrangements accumulate during subsequent mitotic events (Koehler D, Mattes J, Gao J, Joffe B, Cremer T, Eils R, and Solovei I, unpublished data). We do not see any theoretical argument for the evolution of a mechanism that drives full randomization of CT neighborhoods during a single mitotic event. Third, certain differentiation dependent, cell-type specific CT neighborhood arrangements may be maintained in some cycling cell types [11]. The associated mechanism(s) and respective cell cycle stage(s) would require further investigations, but it seems more likely that these would operate during interphase rather than during mitosis. (see Sections 17.6 and 17.7).

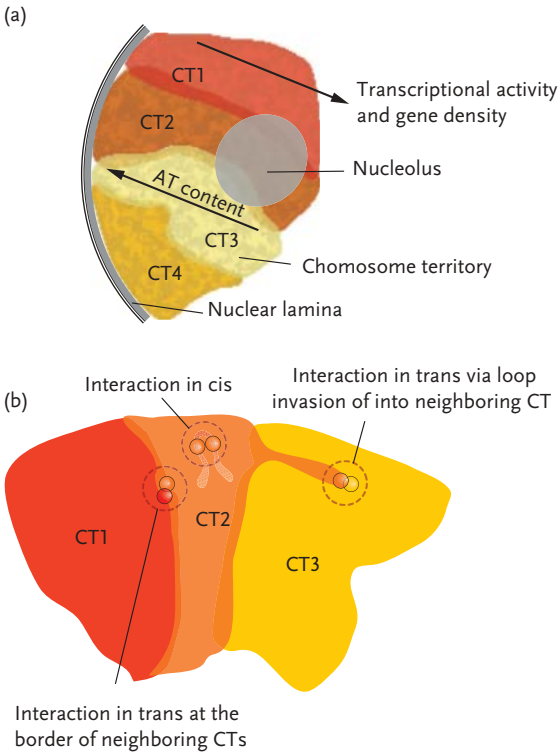

Figure 17.3 Radial nuclear organization of chromatin and spatial interactions between genomic loci in *cis* and *trans*. (a) The relative nuclear position of chromatin contained in a given CT depends on gene density and AT content [16]. (b) Spatial interactions of genes ("gene kissing") in *cis* and *trans* can be explained by the CT-IC model (compare Fig. 17.1) as well as the interchromatin network (ICN) model [56]. A gene kissing event in *trans* is depicted for two genes located at the border zone of CTs 1 and 2. A giant chromatin loop expanding from the surface of CT 2 and penetrating deeply into CT 3 provides another possibility of gene kissing events in *trans*. In addition, CT2 shows a gene kissing event in *cis* between two genes located on the same chromosome, but separated at the DNA sequence level. It has been proposed that gene interactions in *trans* may be triggered between widely separated CTs [127]. If this hypothesis holds true, evidence for a pronounced variability of CT proximity patterns between nuclei from the same cell type [5, 140] implies a necessity for large-scale directed movements of CTs and/or chromatin loops harboring these genes. Alternatively, it seems possible that gene kissing events in *trans* may be restricted to a fraction of nuclei, where the respective genes are already located by chance close enough for interactions driven by locally constrained Brownian movements.

17.6 Large-Scale Chromatin Dynamics in Nuclei of Cycling and Post-Mitotic Cells

Large-scale chromatin movements have received much attention in recent years due to reports that chromatin loci can change nuclear positions over μm distances

and move from a nuclear sub-compartment favorable for silent genes into a neighboring compartment favorable for transcription or *vice versa* [105, 128–130]. Genome-wide mapping approaches yielded strong evidence for multiple, non-random DNA–DNA contacts, mostly in *cis* (as expected as a consequence of CTs) but also in *trans* [44, 131–133]. Such contacts contribute to non-random, cell-type specific features of higher order chromatin organization but the underlying molecular mechanisms remain elusive [56, 65, 134]. Genes located far apart either on the same chromosome or on different chromosomes may come together in the nucleus under certain conditions and spatially associate within a special expression hub or transcription factory (TF) that allows for a co-regulation of associated genes (Figure 17.3) [105, 132, 135]. In the light of findings, which argue for a pronounced variability of neighborhood CT arrangements, such "gene kissing" events may often require positional changes over large distances on the micrometer scale. As discussed in Section 17.4.1 translocations of this magnitude typically do not occur during the observed random movements of a chromatin locus, in which only a region of 200–300 nm diameter is explored. Thus, despite the reports mentioned above that invoke larger positional changes of CDs, chromatin loops and individual genes, the relative location of genome loci with respect to the complete nucleus seems often to be rather stationary in somatic cell types studied to date during interphase.

The relative positioning of a chromosome within the nucleus has been related to gene density and gene expression as well the relative content of DNA segments in GC and AT, respectively [6, 16, 56, 105, 106, 136, 137] (Figure 17.3a). In general, gene-rich CTs locate preferentially in the nuclear interior and gene-poor chromosomes more at the nuclear periphery. As discussed in Chapter 8 an association of chromatin with the nuclear lamina has gene silencing effects. In agreement with this, heterochromatin is enriched in cluster located preferentially at the nuclear periphery and around nucleoli. In line with the increasing evidence that chromatin dynamics play a role at certain stages of cell differentiation, a recent study reported a profound exception to this organization principle [138]. In rod cell nuclei of mammalian species with a nocturnal lifestyle constitutive and facultative heterochromatin forms a single mass in the interior of the nucleus, whereas all transcriptionally active euchromatin locates at the nuclear periphery. This drastic change occurs within a period of several weeks after birth during postmitotic, terminal differentiation of rod cells. Unexpectedly, it was found that rod cell nuclei act as micro-lenses that help to channel light efficiently to the light-sensing rod outer segments. In contrast, rod cell nuclei in diurnal mammalian species show a conventional higher order chromatin organization.

To investigate the positioning of all human CTs in nuclei of fixed primary fibroblasts, Bridger and coworkers employed chromosome painting [139]. They reported major changes of CT arrangements, when a growth arrest was induced in proliferative cells by the removal of serum from the culture medium. These changes became evident in less than 15 min, required ATP, and were inhibited by drugs affecting the polymerization of myosin and actin. When the expression of nuclear myosin 1β was repressed by RNA interference, the induction of CT

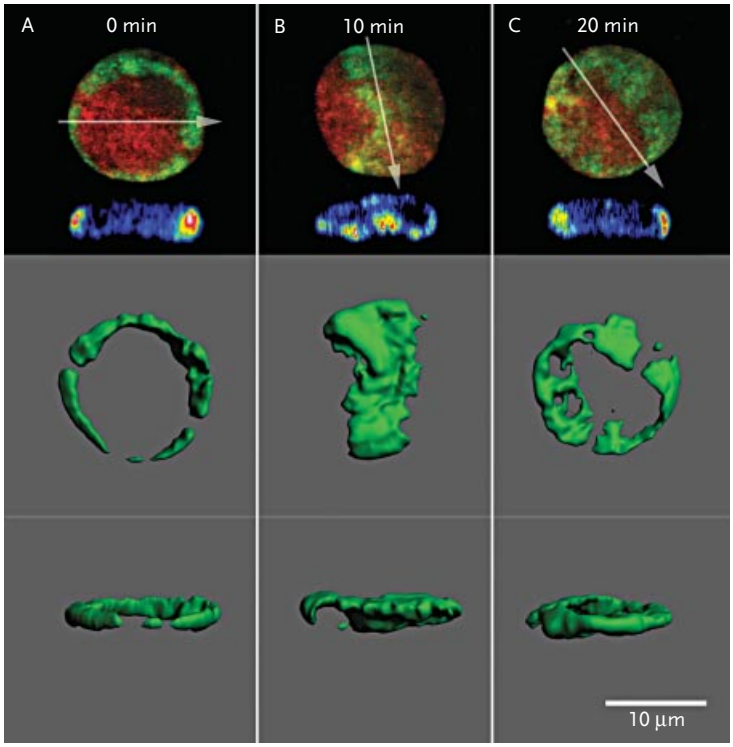

Figure 17.4 Live-cell observation of transient, large-scale changes of CT proximity patterns in a flatly shaped RPE-1 interphase nucleus [5]. The nucleus carried both histone H2B tagged with mRFP (red) and histone H4 tagged with photoactivatable GFP (paGFP-H4). The paGFP fluorescence was activated by illumination at 440 nm around the entire nuclear rim. (a) Image directly after paGFP activation. (b) 10 min later the green ring had apparently turned into a broad band of green fluorescent chromatin expanding across the nucleus. (c) 20 min after paGFP activation a restoration of the fluorescent rim was noted. (a–c) Top row: Projections from stacks of light optical nuclear, serial sections. Below these the nuclear cross-sections along the arrows are shown. Colors from blue to yellow to red indicate increasing intensities of the GFP signal. These cross-sections demonstrate that the photoactivated chromatin remained associated to the nuclear envelope throughout the observation period. Middle and lower rows: 3D reconstructions of the paGFP signal from different viewpoints. The image sequence reveals a rotation of the flatly shaped nucleus around an axis parallel to the growth surface (x,y plane) resulting in a transient change of chromatin proximity patterns (compare Fig. 17.6). This rotation was repeated four times during a total observation period of 110 min (not shown here; compare Figure 3A in [5]). Note that nuclear rotations around an axis perpendicular to the growth surface occurred much more frequently, but did not change chromatin proximity patterns. This rare observation of a nuclear rotation around an axis parallel to the growth surface is likely to reflect corresponding rotational movements of the entire cell. It may be enforced by cytoplasmic filaments attached to the nuclear envelope. Complex rotational, nuclear movements of the type observed here may be part of a mechanism to bring chromatin domains from widely separated CTs in close proximity allowing subsequent "gene kissing" events of genes in *trans* for spatial co-regulation [148] (compare Fig. 17.3b).

movements by low serum was also inhibited. When normal serum concentrations were restored in serum-starved culture, CT repositioning was observed, but required 24–36 h. In support of major changes of CT arrangements occuring on the minute time scale, Strickfaden *et al.* [5] occasionally observed major chromatin movements in nuclei of the human retina pigment epithelium cell line RPE-1. Figure 17.4 depicts such a nucleus after induction of paGFP-H4 fluorescence around the entire nuclear rim. After 10 min the fluorescent chromatin ring had seemingly disappeared. Instead a broad band of fluorescent chromatin expanded from one side of the nucleus to the other. Image sections made in *x,z* through the 3-D image reconstruction of the relatively flat RPE-1 nucleus revealed that the fluorescent chromatin was still associated with the nuclear envelope. However, the CT proximity pattern had largely changed so that some previously separated CTs were brought into close proximity. After 20 min the fluorescent chromatin ring reappeared in the 2-D image projection. This drastic, transient change was repeated four times during the total observation period of 110 min.

These findings point to the need to acquire a more comprehensive and detailed knowledge about chromatin dynamics in nuclei of cycling and post-mitotic living cells. These are particularly important, since conclusions on higher order chromatin arrangements and chromatin dynamics from FISH studies of fixed cell populations could not always be confirmed by later studies [140–142]. The critical issues of FISH procedures and the unbiased, quantitative evaluation of FISH signals in a cell population are discussed in detail in Ref. [143].

17.7
Considerations on Possible Mechanisms of Large-Scale Chromatin Dynamics

The evidence for long-range DNA–DNA interactions in *trans* and large-scale chromatin movements, including entire CTs (see Section 17.6) has prompted a search for the mechanism(s), responsible for the formation of specific higher order chromatin arrangements and their functional implications. These need to account for the randomizing effect of mitosis on CT neighborhood arrangements (see Section 17.5). It seems that probabilistic CT neighborhood arrangements in somatic cell nuclei may be rather the rule than the exception at least in cycling cells [140]. As a caveat we wish to emphasize that most studies of CT arrangements were performed to date with cells cultured *in vitro*. Such studies need to be complemented by systematic, comparative studies of nuclei from various cell types in tissues since the native tissue environment may have profound effects on large scale chromatin dynamics.

It has been proposed that gene kissing events over large distances may be brought about by giant chromatin loops carrying the associated genes to a specialized TF [132]. While these loops clearly exist neither the actual frequency of occurrence nor the organization of giant loops expanding through a major part of the nuclear space is well documented to date. An example for a giant loop structure adapted from Ref. [57] is shown in Figure 17.5. A gene-dense region

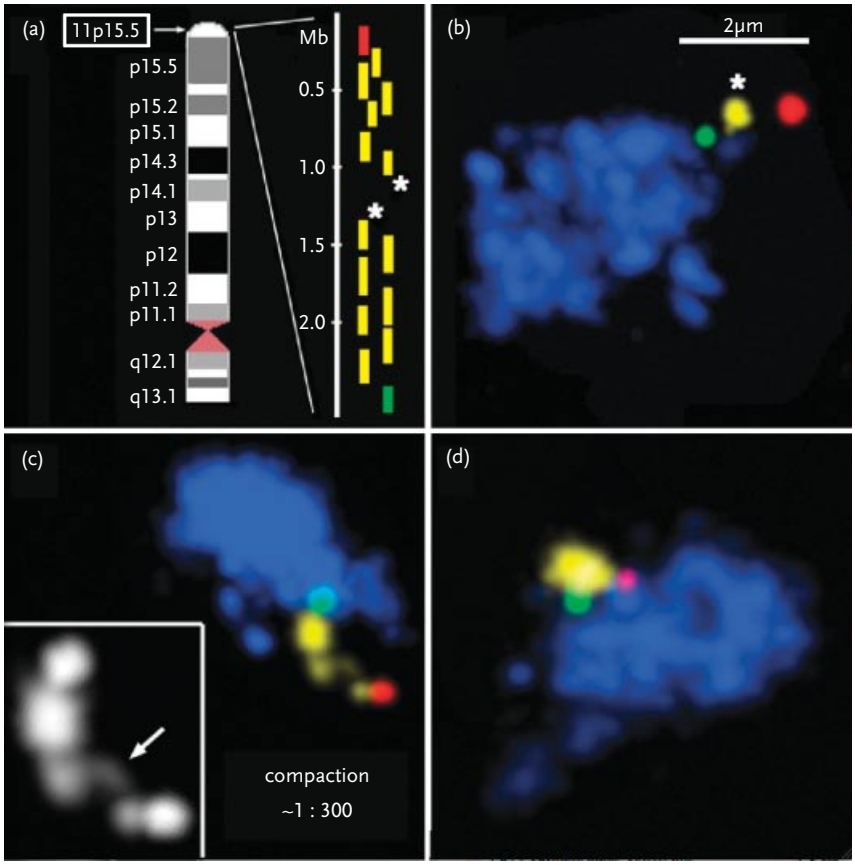

Figure 17.5 Multicolor 3D FISH of a human fibroblast for a 2.34 Mb region on human chromosome locus 11p15.5 (figure taken from ref. [57]). (a) Schematic draft of the 15 bacterial artificial chromosome (BAC) clones used for the contiguous delineation of this region with one 350 kb interruption in the middle. The different colors indicate the most telomeric (red), the most centromeric (green) and the intermediate clones (yellow). (b–d): Maximum intensity projections along the z-axis after 3D-FISH of the CT 11 (blue) and the 11p15.5 BAC probes indicated in the painting scheme. (b) In addition to the two BACs marked green and red, two BACs marked by an asterisk in (a) were visualized together with the CT 11. (c, d) Here, the most telomeric (red) and centromeric (green) BAC were visualized together with all other BACs (yellow). Images in panels (b) and (c) show that the stained region forms a finger-like chromatin protrusion with a compaction factor of ~ 1:300 expanding from CT 11. The inset in (c) outlines the contiguous structure of the region delineated by all BACs. The arrow points to a much thinner fiber segment connecting the thicker parts of the protrusion. (d) Here, the stained region presents itself as a more condensed structure.

located in 11p15.5 with a size of about 2.3 Mb was visualized, which was first described by Mahy *et al.* [144] to expand as a giant loop away from the human CT 11. Whereas Mahy *et al.* used a single BAC for the visualization of this region,

Albiez *et al.* [57] performed multicolor 3-D FISH with a series of BACs extending over the whole region (Figure 17.5).

When tested individually, each BAC yielded a dot-like FISH signal at the periphery or outside the CT. Hybridization with the whole BAC pool allowed the visualization of chromatin configurations ranging from rather compact structures at the CT surface to finger-like chromatin protrusions expanding from the periphery. These had a maximal length of up to 3 μm and a width of several hundred nanometers. The compaction rate of such protrusions was an order of magnitude higher than the compaction ratio of ~1 : 30 to 1 : 40 typical for a 30-nm fiber.

To illustrate the complex demands of long range chromatin movements necessary for kissing events in trans, let us consider the case of the recruitment of specific genes located on two different, randomly arranged CTs for co-regulated expression to a preformed, specialized TF [52, 145, 146]. If this TF is located at a nuclear site remote from these CTs, the respective giant loops must either penetrate through additional CTs located in between or the CTs involved must move aside. While IC channels pervading the nucleus may serve as routes for expanding loops to remote nuclear sites other physical obstacles within the IC due to non-chromatin domains are likely to be present. At the onset of mitosis the retraction of a giant loop towards its corresponding chromosome generates a further potential problem. Most importantly, the directions along which two giant loops expanding from two randomly distributed CTs must move to meet differ strongly in different nuclei. This problem does not exist if efficient transcription of certain genes depends on their spatial interaction with only one of numerous specialized TFs, which are widely distributed throughout the nuclear space. Genes located far away from each other will explore different nuclear sub-volumes and attach to different TFs suitable for their special needs of regulatory factors. However, even probabilistic CT proximity patterns should yield a small fraction of cells, where two or even more genes from the same regulatory gene network, but located on different CTs, attach to the same specialized TF. This would be simply the result of a random localization near enough to attach to the same specialized TF, while they explore their immediate nuclear environment by constrained Brownian motions. Such co-localization events may be more easily discovered by sensitive 3C approaches (Chapter 9). This scenario could explain why 3-D FISH studies of the same cell population typically detect gene co-localization events only in a fraction of nuclei [129].

Complex nuclear rotations may be part of an alternative or additional mechanism with the capacity to generate specific neighborhood arrangements of CTs widely separated prior to such a movement [5]. De Boni and coworkers described saltatory, rotational movements of nuclei with changes in direction [147, 148]. They argued for a link between such complex rotations and the positioning of specific chromatin domains into non-random chromosome pattern in cycling and even in terminal differentiated cells. In multinucleolated neurons studied by time-lapse imaging the same group also observed examples of nucleolar fusion, where nucleoli moved along curvilinear trajectories within the 3-D nuclear space prior to the fusion event [149]. Large-scale movements of nucleoli require concomitant large-scale movements of NOR-bearing CTs and likely also of other CTs carrying

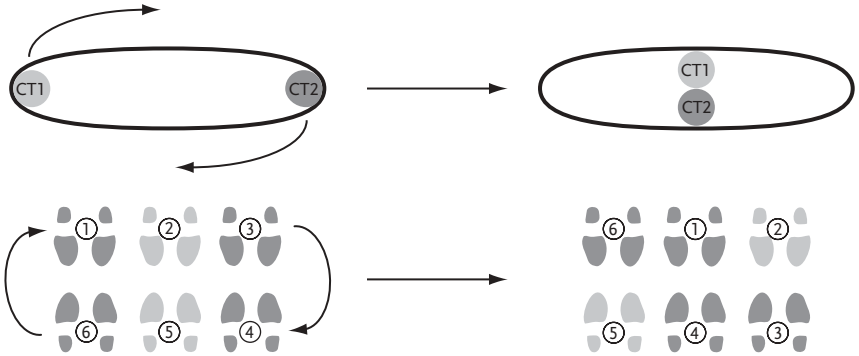

Figure 17.6 Complex rotational movements provide possibilities for the spatial alignment of CTs in somatic cell nuclei. For further details see text.

CDs specifically associated with perinucleolar heterochromatin. Thus, they provide a case in point for the necessity of a choreography, in which CTs move in assemblies rather than as independent individuals. For example, Figure 17.4 shows the rotational movement of the flatly shaped nucleus of a RPE-1 cell studied by live-cell imaging. Changes of CT neighborhoods during rotational nuclear movements around an axis parallel to the growth surface may be compared with a group of square dancers (Figure 17.6).

Importantly, this scenario does not require *a priori* information on the topography of two CTs involved in a "gene kissing" event. For any start configuration a desired pair of dancers can move into a directly opposite position by a clockwise or anti-clockwise rotation of the whole assembly. Figure 17.6 exemplifies only one of many possibilities of changes of CT arrangements brought about by CTs moving in a concerted manner. The larger the diploid number of chromosomes, the more obvious is the need for such a choreography in order to enable positional changes without chaos. The situation of CTs packed together in a nucleus may be compared with the situation in an overcrowded subway wagon. Two persons who are located at opposite sites of the wagon and wish to approach each other are well advised to convince the other passengers to perform coordinated movements similar to the square dance scenario discussed above. The requested nuclear choreography of CTs dancing in assemblies alone still does not suffice to enable gene kissing events. For this purpose additional information is needed, which instructs dancing CTs when to stop. The right moment would be the case, when two CTs largely separated at the beginning of complex nuclear rotation events are close enough to allow a local search driven by constrained Brownian movements. The assumed dance of CTs in assemblies takes place within a 3-D nuclear space. This environment can change shape transiently or permanently. Accordingly, the possibilities for choreographies may be exceedingly more complex than the example of the square dancers shown in Figure 17.6.

Homolog alignment and pairing during meiotic prophase [150] provides a case in point, where coordinated movements of chromosomes in assemblies rather than

isolated movements of individual CTs are required. Another example is somatic homologous chromosome pairing during *Drosophila melanogaster* embryogenesis [151]. Thus, it is tempting to speculate that homologous and heterologous chromatin alignments necessary to achieve a non-random DNA–DNA interaction pattern in *cis* and *trans* also require a concerted movement. The examples mentioned above might all share, at least to some extent, the same molecular mechanisms. These considerations raise the question if rotational movements in the nucleus occur *in toto*, that is, including the nuclear envelope, or whether they represent independent motion of subnuclear structures relative to each other within the nucleus. Reports that CDs showed significant changes of their intranuclear positions while cytoplasmic structures with a juxtanuclear position did not move, suggest that the interface for rotational movements of CT is located on the karyoplasmic side of the nuclear envelope [147]. Rotations of whole nuclei would require a motor fiber system located in the cytoplasm and attached to the nuclear envelope. For intranuclear chromatin rotations such a motor fiber system may either pass from the cytoplasm through the nuclear envelope in order to attach to chromatin sites or the system may be located within the nucleus [139, 152]. In both cases interactions of chromatin with lamin receptors would have to be highly dynamic in order to free peripheral chromatin transiently for rotational movements.

Complex rotational movements of CTs assemblies, followed by constrained Brownian motions of CDs or loops harboring specific genes provide an experimentally testable hypothesis. It predicts how log-range DNA–DNA or chromatin–chromatin interactions *in trans* can be established in a population of cells starting with random CT proximity patterns. In our current view of this process it seems that two separate mechanisms must interact: One mechanism results in the successful alignment of genes, whereas the other mechanism provides the recognition and stabilization of correctly aligned chromatin segments. The latter task may involve chromatin [56, 65, 134] as well as non-chromatin linkers that connects two loci of interest analogous to meiotic transverse filaments [71, 153]. One may even speculate that a kissing event between two genes *in trans* may take place for the first time as a result of complex rotational movements of CT assemblies. Numerous molecular components are likely to be involved in such long-range interactions and remain to be identified. Currently, a few candidates exist: in addition to cytoplasmic and/or nuclear actin and myosin [104, 130, 152, 154, 155] other proteins like dynein [156] should be considered. Furthermore, a disturbance in the connection between the nucleus and the cytoskeleton and a concomitant loss of nuclear rotation was observed in A-type lamin-deficient (lmna–/–) fibroblasts isolated from lmna knockout mice, as well as in 3T3 cells with RNAi induced reduction of lmna expression [157].

Acknowledgment

This work was supported by grants from the Deutsche Forschungsgemeinschaft (DFG).

References

1 Satzinger, H. (2008) Theodor and Marcella Boveri: chromosomes and cytoplasm in heredity and development. *Nat Rev Genet*, **9**, 231–238.

2 Moritz, K.B. and Sauer, H.W. (1996) Boveri's contributions to developmental biology – a challenge for today. *Int J Dev Biol*, **40**, 27–47.

3 Cremer, T. and Cremer, C. (2006) Rise, fall and resurrection of chromosome territories: a historical perspective. Part I. The rise of chromosome territories. *Eur J Histochem*, **50**, 161–176.

4 Cremer, T. and Cremer, C. (2006) Rise, fall and resurrection of chromosome territories: a historical perspective Part II. Fall and resurrection of chromosome territories during the 1950s to 1980s. Part III. Chromosome territories and the functional nuclear architecture: experiments and models from the 1990s to the present. *Eur J Histochem*, **50**, 223–272.

5 Strickfaden, H., Zunhammer, A., van Koningsbruggen, S., Kohler, D., and Cremer, T. (2010) 4D chromatin dynamics in cycling cells: Theodor Boveri's hypotheses revisited. *Nucleus*, **1**, 1–14.

6 Cremer, T., Cremer, M., Dietzel, S., Muller, S., Solovei, I., and Fakan, S. (2006) Chromosome territories – a functional nuclear landscape. *Curr Opin Cell Biol*, **18**, 307–316.

7 Monneron, A. and Bernhard, W. (1969) Fine structural organization of the interphase nucleus in some mammalian cells. *J Ultrastruct Res*, **27**, 266–288.

8 Comings, D.E. (1968) The rationale for an ordered arrangement of chromatin in the interphase nucleus. *Am J Hum Genet*, **20**, 440–460.

9 Comings, D.E. (1980) Arrangement of chromatin in the nucleus. *Hum Genet*, **53**, 131–143.

10 Cremer, T., Kupper, K., Dietzel, S., and Fakan, S. (2004) Higher order chromatin architecture in the cell nucleus: on the way from structure to function. *Biol Cell*, **96**, 555–567.

11 Cremer, T. and Cremer, M. (2010) Chromosome territories. *Cold Spring Harb Persp Biol*, **2**, a003889.

12 Rouquette, J., Cremer, C., Cremer, T., and Fakan, S. (2010) Functional nuclear architecture studied by microscopy: present and future. *Int Rev Cell Mol Biol*, 1–156.

13 Cremer, T. and Cremer, C. (2001) Chromosome territories, nuclear architecture and gene regulation in mammalian cells. *Nat Rev Genet*, **2**, 292–301.

14 Postberg, J., Lipps, H.J., and Cremer, T. (2010) Evolutionary origin of the cell nucleus and its functional architecture. essays in biochemistry: epigenetics, *Dis Behav*, **48**, 1–24.

15 Cremer, T. and Zakhartchenko, V. (2010) Nuclear architecture in developmental biology and cell specialization. *Reprod Fert Develop*, **23**, 94–106.

16 Lanctôt, C., Cheutin, T., Cremer, M., Cavalli, G., and Cremer, T. (2007) Dynamic genome architecture in the nuclear space: regulation of gene expression in three dimensions. *Nat Rev Genet*, **8**, 104–115.

17 van Holde, K.E. (1989) *Chromatin*, Springer, Heidelberg.

18 Bouchet-Marquis, C., Dubochet, J., and Fakan, S. (2006) Cryoelectron microscopy of vitrified sections: a new challenge for the analysis of functional nuclear architecture. *Histochem Cell Biol*, **125**, 43–51.

19 van Holde, K. and Zlatanova, J. (2007) Chromatin fiber structure: where is the problem now? *Semin Cell Dev Biol*, **18**, 651–658.

20 Maeshima, K., Hihara, S., and Eltsov, M. (2010) Chromatin structure: does the 30-nm fibre exist *in vivo*? *Curr Opin Cell Biol*, **22**, 291–297.

21 Ahmed, K., Dehghani, H., Rugg-Gunn, P., Fussner, E., Rossant, J., and Bazett-Jones, D.P. (2010) Global chromatin architecture reflects pluripotency and lineage commitment in the early mouse embryo. *PLoS One*, **5**, e10531.

22 Zentgraf, H. and Franke, W.W. (1984) Differences of supranucleosomal organization in different kinds of chromatin: cell type-specific globular subunits containing different numbers of nucleosomes. *J Cell Biol*, **99**, 272–286.

23 Hansen, J.C. (2002) Conformational dynamics of the chromatin fiber in solution: determinants, mechanisms, and functions. *Annu Rev Biophys Biomol Struct*, **31**, 361–392.

24 Woodcock, C.L. (2006) Chromatin architecture. *Curr Opin Struct Biol*, **16**, 213–220.

25 Robinson, P.J. and Rhodes, D. (2006) Structure of the "30 nm" chromatin fibre: a key role for the linker histone. *Curr Opin Struct Biol*, **16**, 336–343.

26 Belmont, A.S. and Bruce, K. (1994) Visualization of G1 chromosomes: a folded, twisted, supercoiled chromonema model of interphase chromatid structure. *J Cell Biol*, **127**, 287–302.

27 Belmont, A.S., Braunfeld, M.B., Sedat, J.W., and Agard, D.A. (1989) Large-scale chromatin structural domains within mitotic and interphase chromosomes *in vivo* and *in vitro*. *Chromosoma*, **98**, 129–143.

28 Tumbar, T., Sudlow, G., and Belmont, A.S. (1999) Large-scale chromatin unfolding and remodeling induced by VP16 acidic activation domain. *J Cell Biol*, **145**, 1341–1354.

29 Hahnfeldt, P., Hearst, J.E., Brenner, D. J., Sachs, R.K., and Hlatky, L.R. (1993) Polymer models for interphase chromosomes. *Proc Natl Acad Sci USA*, **90**, 7854–7858.

30 McDowall, A.W., Smith, J.M., and Dubochet, J. (1986) Cryo-electron microscopy of vitrified chromosomes *in situ*. *EMBO J*, **5**, 1395–1402.

31 Maeshima, K. and Eltsov, M. (2008) Packaging the genome: the structure of mitotic chromosomes. *J Biochem*, **143**, 145–153.

32 Rosa, A. and Everaers, R. (2008) Structure and dynamics of interphase chromosomes. *PLoS Comput biology*, **4**, e1000153.

33 Rosa, A., Becker, N.B., and Everaers, R. (2010) Looping probabilities in model interphase chromosomes. *Biophys J*, **98**, 2410–2419.

34 Ostashevsky, J.Y. and Lange, C.S. (1994) The 30 nm chromatin fiber as a flexible polymer. *J Biomol Struct Dyn*, **11**, 813–820.

35 Sachs, R.K., van den Engh, G., Trask, B., Yokota, H., and Hearst, J.E. (1995) A random-walk/giant-loop model for interphase chromosomes. *Proc Natl Acad Sci USA*, **92**, 2710–2714.

36 Ostashevsky, J. (2002) A polymer model for large-scale chromatin organization in lower eukaryotes. *Mol Biol Cell*, **13**, 2157–2169.

37 Hamkalo, B.A. and Rattner, J.B. (1980) Folding up genes and chromosomes. *Q Rev Biol*, **55**, 409–417.

38 Pienta, K.J. and Coffey, D.S. (1984) A structural analysis of the role of the nuclear matrix and DNA loops in the organization of the nucleus and chromosome. *J Cell Sci Suppl*, **1**, 123–135.

39 Münkel, C., Eils, R., Dietzel, S., Zink, D., Mehring, C., Wedemann, G., Cremer, T., and Langowski, J. (1999) Compartmentalization of interphase chromosomes observed in simulation and experiment. *J Mol Biol*, **285**, 1053–1065.

40 Paul, A.L., and Ferl, R.J. (1999) Higher-order chromatin structure: looping long molecules. *Plant Mol Biol*, **41**, 713–720.

41 Bohn, M., Heermann, D.W., and van Driel, R. (2007) Random loop model for long polymers. *Phys Rev E Stat Nonlinear Soft Matter Phys*, **76**, 051805.

42 Mateos-Langerak, J., Bohn, M., de Leeuw, W., Giromus, O., Manders, E. M., Verschure, P.J., Indemans, M.H., Gierman, H.J., Heermann, D.W., van Driel, R., and Goetze, S. (2009) Spatially confined folding of chromatin in the interphase nucleus. *Proc Natl Acad Sci USA*, **106**, 3812–3817.

43 Takahashi, M. (1989) A fractal model of chromosomes and chromosomal DNA replication. *J Theor Biol*, **141**, 117–136.

44 Lieberman-Aiden, E., van Berkum, N. L., Williams, L., Imakaev, M., Ragoczy,

T., Telling, A., Amit, I., Lajoie, B.R., Sabo, P.J., Dorschner, M.O., Sandstrom, R., *et al.* (2009) Comprehensive mapping of long-range interactions reveals folding principles of the human genome. *Science*, **326**, 289–293.

45 Schermelleh, L., Solovei, I., Zink, D., and Cremer, T. (2001) Two-color fluorescence labeling of early and mid-to-late replicating chromatin in living cells, *Chromosome Res*, **9**, 77–80.

46 Baddeley, D., Chagin, V.O., Schermelleh, L., Martin, S., Pombo, A., Carlton, P.M., Gahl, A., Domaing, P., Birk, U., Leonhardt, H., Cremer, C., *et al.* (2010) Measurement of replication structures at the nanometer scale using super-resolution light microscopy. *Nucleic Acids Res*, **38**, e8.

47 Zink, D., Bornfleth, H., Visser, A., Cremer, C., and Cremer, T. (1999) Organization of early and late replicating DNA in human chromosome territories. *Exp Cell Res*, **247**, 176–188.

48 Berezney, R., Dubey, D.D., and Huberman, J.A. (2000) Heterogeneity of eukaryotic replicons, replicon clusters, and replication foci. *Chromosoma*, **108**, 471–484.

49 Visser, A.E., Jaunin, F., Fakan, S., and Aten, J.A. (2000) High resolution analysis of interphase chromosome domains. *J Cell Sci*, **113** (Pt 14), 2585–2593.

50 Müller, W.G., Rieder, D., Kreth, G., Cremer, C., Trajanoski, Z., and McNally, J.G. (2004) Generic features of tertiary chromatin structure as detected in natural chromosomes. *Mol Cell Biol*, **24**, 9359–9370.

51 Fakan, S. and van Driel, R. (2007) The perichromatin region: a functional compartment in the nucleus that determines large-scale chromatin folding. *Semin Cell Dev Biol*, **18**, 676–681.

52 Chakalova, L. and Fraser, P. (2010) Organization of transcription. *Cold Spring Harb Perspect Biol*, **2**, a000729.

53 Lichter, P., Cremer, T., Borden, J., Manuelidis, L., and Ward, D.C. (1988) Delineation of individual human chromosomes in metaphase and interphase cells by *in situ* suppression hybridization using recombinant DNA libraries. *Hum Genet*, **80**, 224–234.

54 Pinkel, D., Landegent, J., Collins, C., Fuscoe, J., Segraves, R., Lucas, J., and Gray, J. (1988) Fluorescence *in situ* hybridization with human chromosome-specific libraries: detection of trisomy 21 and translocations of chromosome 4. *Proc Natl Acad Sci USA*, **85**, 9138–9142.

55 Cremer, T., Kurz, A., Zirbel, R., Dietzel, S., Rinke, B., Schrock, E., Speicher, M.R., Mathieu, U., Jauch, A., Emmerich, P., Scherthan, H., *et al.* (1993) Role of chromosome territories in the functional compartmentalization of the cell nucleus. *Cold Spring Harb Symp Quant Biol*, **58**, 777–792.

56 Branco, M. and Pombo, A. (2007) Chromosome organization: new facts, new models. *Trends Cell Biol*, **17**, 127–134.

57 Albiez, H., Cremer, M., Tiberi, C., Vecchio, L., Schermelleh, L., Dittrich, S., Küpper, K., Joffe, B., Thormeyer, T., Hase, J., Yang, S., *et al.* (2006) Chromatin domains and the interchromatin compartment form structurally defined and functionally interacting nuclear networks, *Chromosome Res*, **14**, 707–733.

58 Rouquette, J., Genoud, C., Vazquez-Nin, G.H., Kraus, B., Cremer, T., and Fakan, S. (2009) Revealing the high-resolution three-dimensional network of chromatin and interchromatin space: a novel electron-microscopic approach to reconstructing nuclear architecture. *Chromosome Res*, **17**, 801–810.

59 Zirbel, R.M., Mathieu, U.R., Kurz, A., Cremer, T., and Lichter, P. (1993) Evidence for a nuclear compartment of transcription and splicing located at chromosome domain boundaries. *Chromosome Res*, **1**, 93–106.

60 Reichenzeller, M., Burzlaff, A., Lichter, P., and Herrmann, H. (2000) *In vivo* observation of a nuclear channel-like system: evidence for a distinct interchromosomal domain compartment in interphase cells. *J Struct Biol*, **129**, 175–185.

61 Herrmann, H. and Lichter, P. (1999) New ways to look at the interchromosomal-domain compartment. *Protoplasma*, **209**, 157–165.

62 Bridger, J.M., Herrmann, H., Münkel, C., and Lichter, P. (1998) Identification of an interchromosomal compartment by polymerization of nuclear-targeted vimentin. *J Cell Sci*, **111** (Pt 9), 1241–1253.

63 Scheuermann, M.O., Murmann, A.E., Richter, K., Gorisch, S.M., Herrmann, H., and Lichter, P. (2005) Characterization of nuclear compartments identified by ectopic markers in mammalian cells with distinctly different karyotype. *Chromosoma*, **114**, 39–53.

64 Richter, K., Reichenzeller, M., Görisch, S.M., Schmidt, U., Scheuermann, M. O., Herrmann, H., and Lichter, P. (2005) Characterization of a nuclear compartment shared by nuclear bodies applying ectopic protein expression and correlative light and electron microscopy. *Exp Cell Res*, **303**, 128–137.

65 Marenduzzo, D., Faro-Trindade, I., and Cook, P. (2007) What are the molecular ties that maintain genomic loops? *Trends Genet*, **23**, 126–133.

66 Görisch, S.M., Lichter, P., and Rippe, K. (2005) Mobility of multi-subunit complexes in the nucleus: chromatin dynamics and accessibility of nuclear subcompartments. *Histochem Cell Biol*, **123**, 217–228.

67 Görisch, S.M., Wachsmuth, M., Ittrich, C., Bacher, C.P., Rippe, K., and Lichter, P. (2004) Nuclear body movement is determined by chromatin accessibility and dynamics. *Proc Natl Acad Sci USA*, **101**, 13221–13226.

68 Cmarko, D., Verschure, P.J., Martin, T. E., Dahmus, M.E., Krause, S., Fu, X.D., Van Driel, R., and Fakan, S. (1999) Ultrastructural analysis of transcription and splicing in the cell nucleus after bromo-UTP microinjection, *Mol Biol Cell*, **10**, 211–223.

69 Cmarko, D., Verschure, P.J., Otte, A.P., van Driel, R., and Fakan, S. (2003) Polycomb group gene silencing proteins are concentrated in the perichromatin compartment of the mammalian nucleus, *J Cell Sci*, **116**, 335–343.

70 Solimando, L., Luijsterburg, M.S., Vecchio, L., Vermeulen, W., Van Driel, R., and Fakan, S. (2009) Spatial organization of nucleotide excision repair proteins after UV-induced DNA damage in the human cell nucleus, *J Cell Sci*, **122**, 83–91.

71 Markaki, Y., Gunkel, M., Schermelleh, L., Beichmanis, S., Neumann, J., Heidemann, M., Leonhardt, H., Eick, D., Cremer, C., and Cremer, T. (2010) Functional nuclear organization of transcription and DNA replication. A topographical marriage between chromatin domains and the interchromatin compartment. *Cold Spring Harb Symp Quan Biol: Nuclear Org Funct*, **75**, 475–492.

72 Branco, M. and Pombo, A. (2006) Intermingling of chromosome territories in interphase suggests role in translocations and transcription-dependent associations. *PLoS Biol*, **4**, e138.

73 Kreth, G., Munkel, C., Langowski, J., Cremer, T., and Cremer, C. (1998) Chromatin structure and chromosome aberrations: modeling of damage induced by isotropic and localized irradiation. *Mut Res Fund Mol Mech Mut*, **404**, 77–88.

74 Kreth, G., Pazhanisamy, S.K., Hausmann, M., and Cremer, C. (2007) Cell type-specific quantitative predictions of radiation-induced chromosome aberrations: a computer model approach. *Radiat Res*, **167**, 515–525.

75 Gerchman, S.E. and Ramakrishnan, V. (1987) Chromatin higher-order structure studied by neutron scattering and scanning transmission electron microscopy. *Proc Natl Acad Sci USA*, **84**, 7802–7806.

76 Ghirlando, R. and Felsenfeld, G. (2008) Hydrodynamic studies on defined heterochromatin fragments support a 30-nm fiber having six nucleosomes per turn. *J Mol Biol*, **376**, 1417–1425.

77 Weidemann, T., Wachsmuth, M., Knoch, T., Müller, G., Waldeck, W., and Langowski, J. (2003) Counting nucleosomes in living cells with a combination of fluorescence correlation spectroscopy and confocal imaging. *J Mol Biol*, **334**, 229–240.

78 Zeskind, B.J., Jordan, C.D., Timp, W., Trapani, L., Waller, G., Horodincu, V., Ehrlich, D.J., and Matsudaira, P. (2007) Nucleic acid and protein mass mapping by live-cell deep-ultraviolet microscopy. *Nat Methods*, **4**, 567–569.

79 Görisch, S., Wachsmuth, M., Fejes Tóth, K., Lichter, P., and Rippe, K. (2005) Histone acetylation increases chromatin accessibility. *J Cell Sci*, **118**, 5825–5834.

80 Wachsmuth, M., Caudron-Herger, M., and Rippe, K. (2008) Genome organization: balancing stability and plasticity. *Biochim Biophys Acta*, **1783**, 2061–2079.

81 Rego, A., Sinclair, P.B., Tao, W., Kireev, I., and Belmont, A.S. (2008) The facultative heterochromatin of the inactive X chromosome has a distinctive condensed ultrastructure. *J Cell Sci*, **121**, 1119–1127.

82 Fejes Tóth, K., Knoch, T.A., Wachsmuth, M., Stöhr, M., Frank-Stöhr, M., Bacher, C.P., Müller, G., and Rippe, K. (2004) Trichostatin A induced histone acetylation causes decondensation of interphase chromatin. *J Cell Sci*, **117**, 4277–4287.

83 Janicki, S.M., Tsukamoto, T., Salghetti, S.E., Tansey, W.P., Sachidanandam, R., Prasanth, K.V., Ried, T., Shav-Tal, Y., Bertrand, E., Singer, R.H., and Spector, D.L. (2004) From silencing to gene expression: real-time analysis in single cells. *Cell*, **116**, 683–698.

84 Richter, K., Nessling, M., and Lichter, P. (2007) Experimental evidence for the influence of molecular crowding on nuclear architecture. *J Cell Sci*.

85 Verschure, P.J., van der Kraan, I., Manders, E.M., Hoogstraten, D., Houtsmuller, A.B., and van Driel, R. (2003) Condensed chromatin domains in the mammalian nucleus are accessible to large macromolecules. *EMBO Rep*, **4**, 861–866.

86 Pack, C., Saito, K., Tamura, M., and Kinjo, M. (2006) Microenvironment and effect of energy depletion in the nucleus analyzed by mobility of multiple oligomeric EGFPs. *Biophys J*, **91**, 3921–3936.

87 Görisch, S.M., Richter, K., Scheuermann, M.O., Herrmann, H., and Lichter, P. (2003) Diffusion-limited compartmentalization of mammalian cell nuclei assessed by microinjected macromolecules, *Exp Cell Res*, **289**, 282–294.

88 Tseng, Y., Lee, J.S., Kole, T.P., Jiang, I., and Wirtz, D. (2004) Micro-organization and visco-elasticity of the interphase nucleus revealed by particle nanotracking, *J Cell Sci*, **117**, 2159–2167.

89 Wachsmuth, M., Waldeck, W., and Langowski, J. (2000) Anomalous diffusion of fluorescent probes inside living cell nuclei investigated by spatially-resolved fluorescence correlation spectroscopy. *J Mol Biol*, **298**, 677–689.

90 Beaudouin, J., Mora-Bermúdez, F., Klee, T., Daigle, N., and Ellenberg, J. (2006) Dissecting the contribution of diffusion and interactions to the mobility of nuclear proteins. *Biophys J*, **90**, 1878–1894.

91 Abney, J.R., Cutler, B., Fillbach, M.L., Axelrod, D., and Scalettar, B.A. (1997) Chromatin dynamics in interphase nuclei and its implications for nuclear structure. *J Cell Biol*, **137**, 1459–1468.

92 Robinett, C.C., Straight, A., Li, G., Willhelm, C., Sudlow, G., Murray, A., and Belmont, A.S. (1996) *In vivo* localization of DNA sequences and visualization of large-scale chromatin organization using lac operator/repressor recognition, 135.

93 Chuang, C.H., and Belmont, A.S. (2007) Moving chromatin within the interphase nucleus-controlled transitions? *Semin Cell Dev Biol*, **18**, 698–706.

94 Chubb, J.R., Boyle, S., Perry, P., and Bickmore, W.A. (2002) Chromatin

motion is constrained by association with nuclear compartments in human cells, *Curr Biol*, **12**, 439–445.

95 Levi, V., Ruan, Q., Plutz, M., Belmont, A., and Gratton, E. (2005) Chromatin dynamics in interphase cells revealed by tracking in a two-photon excitation microscope. *Biophys J*, **89**, 4275–4285.

96 Soutoglou, E., Dorn, J., Sengupta, K., Jasin, M., Nussenzweig, A., Ried, T., Danuser, G., and Misteli, T. (2007) Positional stability of single double-strand breaks in mammalian cells. *Nat Cell Biol*, **9**, 675–682.

97 De Vos, W.H., Houben, F., Hoebe, R. A., Hennekam, R., Van Engelen, B., Manders, E.M.M., Ramaekers, F.C.S., Broers, J.L.V., and Van Oostveldt, P. (2010) Increased plasticity of the nuclear envelope and hypermobility of telomeres due to the loss of A–type lamins. *Biochim Biophys Acta (BBA) – Gen Sub*, **1800**, 448–458.

98 Jegou, T., Chung, I., Heuvelmann, G., Wachsmuth, M., Görisch, S.M., Greulich-Bode, K., Boukamp, P., Lichter, P., and Rippe, K. (2009) Dynamics of telomeres and promyelocytic leukemia nuclear bodies in a telomerase negative human cell line. *Mol Biol Cell*, **20**, 2070–2082.

99 Bronstein, I., Israel, Y., Kepten, E., Mai, S., Shav-Tal, Y., Barkai, E., and Garini, Y. (2009) Transient anomalous diffusion of telomeres in the nucleus of mammalian cells. *Phys Rev Lett*, **103**, 018102.

100 Wang, X., Kam, Z., Carlton, P.M., Xu, L., Sedat, J.W., and Blackburn, E.H. (2008) Rapid telomere motions in live human cells analyzed by highly time-resolved microscopy. *Epigenet Chroma*, **1**, 4.

101 Dimitrova, N., Chen, Y.-C.M., Spector, D.L., and De Lange, T. (2008) 53BP1 promotes non-homologous end joining of telomeres by increasing chromatin mobility. *Nature*, **456**, 524–528.

102 Molenaar, C., Wiesmeijer, K., Verwoerd, N.P., Khazen, S., Eils, R., Tanke, H.J., and Dirks, R.W. (2003) Visualizing telomere dynamics in living mammalian cells using PNA probes, *EMBO J*, **22**, 6631–6641.

103 Bornfleth, H., Edelmann, P., Zink, D., Cremer, T., and Cremer, C. (1999) Quantitative motion analysis of subchromosomal foci in living cells using four-dimensional microscopy. *Biophys J*, **77**, 2871–2886.

104 Chuang, C., Carpenter, A., Fuchsova, B., Johnson, T., de Lanerolle, P., and Belmont, A. (2006) Long-range directional movement of an interphase chromosome site. *Curr Biol*, **16**, 825–831.

105 Fraser, P. and Bickmore, W. (2007) Nuclear organization of the genome and the potential for gene regulation. *Nature*, **447**, 413–417.

106 Misteli, T. (2007) Beyond the sequence: cellular organization of genome function. *Cell*, **128**, 787–800.

107 Doi, M. and Edwards, S.F. (1986) *The Theory of Polymer Dynamics*, Oxford University Press, Oxford.

108 Platani, M., Goldberg, I., Lamond, A.I., and Swedlow, J.R. (2002) Cajal body dynamics and association with chromatin are ATP-dependent, *Nat Cell Biol*, **4**, 502–508.

109 Muratani, M., Gerlich, D., Janicki, S. M., Gebhard, M., Eils, R., and Spector, D.L. (2002) Metabolic-energy-dependent movement of PML bodies within the mammalian cell nucleus, *Nat Cell Biol*, **4**, 106–110.

110 Handwerger, K.E., Murphy, C., and Gall, J.G. (2003) Steady-state dynamics of Cajal body components in the *Xenopus* germinal vesicle. *J Cell Biol*, **160**, 495–504.

111 Weidtkamp-Peters, S., Lenser, T., Negorev, D., Gerstner, N., Hofmann, T.G., Schwanitz, G., Hoischen, C., Maul, G., Dittrich, P., and Hemmerich, P. (2008) Dynamics of component exchange at PML nuclear bodies. *J Cell Sci*, **121**, 2731–2743.

112 Handwerger, K. and Gall, J. (2006) Subnuclear organelles: new insights into form and function. *Trends Cell Biol*, **16**, 19–26.

113 Lamond, A.I. and Spector, D.L. (2003) Nuclear speckles: a model for nuclear organelles. *Nat Rev Mol Cell Biol*, **4**, 605–612.

114 Frey, M.R. and Matera, A.G. (1995) Coiled bodies contain U7 small nuclear RNA and associate with specific DNA sequences in interphase human cells, *Proc Natl Acad Sci USA*, **92**, 5915–5919.

115 Schul, W., van Driel, R., and de Jong, L. (1998) Coiled bodies and U2 snRNA genes adjacent to coiled bodies are enriched in factors required for snRNA transcription, *Mol Biol Cell*, **9**, 1025–1036.

116 Jacobs, E.Y., Frey, M.R., Wu, W., Ingledue, T.C., Gebuhr, T.C., Gao, L., Marzluff, W.F., and Matera, A.G. (eds.) (1999) Coiled bodies preferentially associate with U4, U11, and U12 small nuclear RNA genes in interphase HeLa cells but not with U6 and U7 genes.

117 Gall, J.G., Stephenson, E.C., Erba, H. P., Diaz, M.O., and Barsacchi-Pilone, G. (1981) Histone genes are located at the sphere loci of newt lampbrush chromosomes, *Chromosoma*, **84**, 159–171.

118 Callan, H.G., Gall, J.G., and Murphy, C. (1991) Histone genes are located at the sphere loci of *Xenopus* lampbrush chromosomes. *Chromosoma*, **101**, 245–251.

119 Shiels, C., Islam, S.A., Vatcheva, R., Sasieni, P., Sternberg, M.J., Freemont, P.S., and Sheer, D. (2001) PML bodies associate specifically with the MHC gene cluster in interphase nuclei. *J Cell Sci*, **114**, 3705–3716.

120 Wang, J., Shiels, C., Sasieni, P., Wu, P. J., Islam, S.A., Freemont, P.S., and Sheer, D. (2004) Promyelocytic leukemia nuclear bodies associate with transcriptionally active genomic regions. *J Cell Biol*, **164**, 515–526.

121 Yeager, T.R., Neumann, A.A., Englezou, A., Huschtscha, L.I., Noble, J.R., and Reddel, R.R. (1999) Telomerase-negative immortalized human cells contain a novel type of promyelocytic leukemia (PML) body. *Cancer Res*, **59**, 4175–4179.

122 Gerlich, D., Beaudouin, J., Kalbfuss, B., Daigle, N., Eils, R., and Ellenberg, J. (2003) Global chromosome positions are transmitted through mitosis in mammalian cells. *Cell*, **112**, 751–764.

123 Walter, J., Schermelleh, L., Cremer, M., Tashiro, S., and Cremer, T. (2003) Chromosome order in HeLa cells changes during mitosis and early G1, but is stably maintained during subsequent interphase stages. *J Cell Biol*, **160**, 685–697.

124 Cvackova, Z., Masata, M., Stanek, D., Fidlerova, H., and Raska, I. (2009) Chromatin position in human HepG2 cells: although being non-random, significantly changed in daughter cells. *J Struct Biol*, **165**, 107–117.

125 Wiesmeijer, K., Krouwels, I.M., Tanke, H.J., and Dirks, R.W. (2007) Chromatin movement visualized with photoactivable GFP-labeled histone H4. Differentiation.

126 Thomson, I., Gilchrist, S., Bickmore, W.A., and Chubb, J.R. (2004) The radial positioning of chromatin is not inherited through mitosis but is established *de novo* in early G1. *Curr Biol*, **14**, 166–172.

127 Nunez, E., Fu, X.-D., and Rosenfeld, M.G. (2009) Nuclear organization in the 3D space of the nucleus – cause or consequence? *Curr Opin Genet Dev*, **19**, 424–436.

128 Lin, C., Yang, L., Tanasa, B., Hutt, K., Ju, B.-G., Ohgi, K., Zhang, J., Rose, D. W., Fu, X.-D., Glass, C.K., and Rosenfeld, M.G. (2009) Nuclear receptor-induced chromosomal proximity and DNA breaks underlie specific translocations in cancer, *Cell*, **139**, 1069–1083.

129 Schoenfelder, S., Sexton, T., Chakalova, L., Cope, N.F., Horton, A., Andrews, S., Kurukuti, S., Mitchell, J.A., Umlauf, D., Dimitrova, D.S., Eskiw, C.H., *et al.* (2010) Preferential associations between co-regulated genes reveal a transcriptional interactome in erythroid cells. *Nat Genet*, **42**, 53–61.

130 Hu, Q., Kwon, Y.-S., Nunez, E., Cardamone, M.D., Hutt, K.R., Ohgi, K. A., Garcia-Bassets, I., Rose, D.W., Glass, C.K., Rosenfeld, M.G., and Fu,

X.-D. (2008) Enhancing nuclear receptor-induced transcription requires nuclear motor and LSD1-dependent gene networking in interchromatin granules, *Proc Natl Acad Sci*, **105**, 19199–19204.

131 van Steensel, B. and Dekker, J. (2010) Genomics tools for unraveling chromosome architecture. *Nat Biotechnol*, **28**, 1089–1095.

132 Göndör, A. and Ohlsson, R. (2009) Chromosome crosstalk in three dimensions. *Nature*, **461**, 212–217.

133 Hakim, O., Sung, M.H., and Hager, G. L. (2010) 3D shortcuts to gene regulation. *Curr Opin Cell Biol*, **22**, 305–313.

134 Rippe, K. (2007) Dynamic organization of the cell nucleus. *Curr Opin Genet Dev*, **17**, 373–380.

135 Kosak, S.T. and Groudine, M. (2004) Form follows function: the genomic organization of cellular differentiation. *Genes Dev*, **18**, 1371–1384.

136 Foster, H.A. and Bridger, J.M. (2005) The genome and the nucleus: a marriage made by evolution. Genome organisation and nuclear architecture. *Chromosoma*, **114**, 212–229.

137 Sexton, T., Schober, H., Fraser, P., and Gasser, S.M. (2007) Gene regulation through nuclear organization. *Nat Struct Mol Biol*, **14**, 1049–1055.

138 Solovei, I., Kreysing, M., Lanctot, C., Kosem, S., Peichl, L., Cremer, T., Guck, J., and Joffe, B. (2009) Nuclear architecture of rod photoreceptor cells adapts to vision in mammalian evolution. *Cell*, **137**, 356–368.

139 Mehta, I.S., Amira, M., Harvey, A.J., and Bridger, J.M. (2010) Rapid chromosome territory relocation by nuclear motor activity in response to serum removal in primary human fibroblasts. *Genome Biol*, **11**, R5.

140 Bolzer, A., Kreth, G., Solovei, I., Koehler, D., Saracoglu, K., Fauth, C., Müller, S., Eils, R., Cremer, C., Speicher, M., and Cremer, T. (2005) Three-dimensional maps of all chromosomes in human male fibroblast nuclei and prometaphase rosettes. *PLoS Biol*, **3**, e157.

141 Teller, K., Solovei, I., Buiting, K., Horsthemke, B., and Cremer, T. (2007) Maintenance of imprinting and nuclear architecture in cycling cells. *Proc Natl Acad Sci USA*, **104**, 14970–14975.

142 Kocanova, S., Kerr, E.A., Rafique, S., Boyle, S., Katz, E., Caze-Subra, S., Bickmore, W.A., and Bystricky, K. (2010) Activation of estrogen-responsive genes does not require their nuclear co-localization. *PLoS Genet*, **6**, e1000922.

143 Ronneberger, O., Baddeley, D., Scheipl, F., Verveer, P.J., Burkhardt, H., Cremer, C., Fahrmeir, L., Cremer, T., and Joffe, B. (2008) Spatial quantitative analysis of fluorescently labeled nuclear structures: problems, methods, pitfalls. *Chromosome Res*, **16**, 523–562.

144 Mahy, N.L., Perry, P.E., and Bickmore, W.A. (2002) Gene density and transcription influence the localization of chromatin outside of chromosome territories detectable by FISH. *J Cell Biol*, **159**, 753–763.

145 Xu, M., and Cook, P.R. (2008) The role of specialized transcription factories in chromosome pairing. *Biochim Biophys Acta*, **1783**, 2155–2160.

146 Cook, P.R. (2010) A model for all genomes: the role of transcription factories. *J Mol Biol*, **395**, 1–10.

147 De Boni, U. and Mintz, A.H. (1986) Curvilinear, three-dimensional motion of chromatin domains and nucleoli in neuronal interphase nuclei. *Science*, **234**, 863–866.

148 De Boni, U. (1988) Chromatin motion in interphase nuclei, its modulation and its potential role in gene expression, *Anticancer Res*, **8**, 885–898.

149 Park, P.C. and De Boni, U. (1991) Dynamics of nucleolar fusion in neuronal interphase nuclei *in vitro*: association with nuclear rotation. *Exp Cell Res*, **197**, 213–221.

150 Moore, G. and Shaw, P. (2009) Improving the chances of finding the right partner, *Curr Opin Genet Dev*, **19**, 99–104.

151 Hiraoka, Y., Dernburg, A.F., Parmelee, S.J., Rykowski, M.C., Agard, D.A., and Sedat, J.W. (1993) The onset of

homologous chromosome pairing during *Drosophila melanogaster* embryogenesis, *J Cell Biol*, **120**, 591–600.

152 Mehta, I.S., Elcock, L.S., Amira, M., Kill, I.R., and Bridger, J.M. (2008) Nuclear motors and nuclear structures containing A-type lamins and emerin: is there a functional link? *Biochem Soc Trans*, **36**, 1384–1388.

153 Heyting, C. (2005) Meiotic transverse filament proteins: essential for crossing over, *Transgenic Res*, **14**, 547–550.

154 Pederson, T. (2008) As functional nuclear actin comes into view, is it globular, filamentous, or both?, *J Cell Biol*, **180**, 1061–1064.

155 Pederson, T. and Aebi, U. (2005) Nuclear actin extends, with no contraction in sight, *Mol Biol Cell*, **16**, 5055–5060.

156 Levy, J.R. and Holzbaur, E.L.F. (2008) Dynein drives nuclear rotation during forward progression of motile fibroblasts, *J Cell Sci*, **121**, 3187–3195.

157 Houben, F., Willems, C.H.M.P., Declercq, I.L.J., Hochstenbach, K., Kamps, M.A., Snoeckx, L.H.E.H., Ramaekers, F.C.S., and Broers, J.L.V. (2009) Disturbed nuclear orientation and cellular migration in A-type lamin deficient cells, *Biochim Biophys Acta*, **1793**, 312–324.